JOURNAL OF CATALYSIS **168,** 292–300 (1997)
ARTICLE NO. CA971655

Improving the Stability of H–Mordenite for *n*-Butane Isomerization

R. A. Asuquo, G. Eder-Mirth, K. Seshan, J. A. Z. Pieterse, and J. A. Lercher

Faculty of Chemical Technology and the Christian Doppler Laboratory for Heterogeneous Catalysis, University of Twente, P.O. Box 217, 7500 AE Enschede, The Netherlands

Received March 14, 1996; revised February 10, 1997; accepted February 13, 1997

The conversion of *n*-butane over mordenite-based catalysts in the presence of hydrogen and water was investigated for reaction temperatures between 523 and 623 K. Special attention was given to the influence of Pt upon catalytic activity, selectivity, and stability. With parent mordenite the catalytic activity for *n*-butane conversion decreased markedly after a short time on stream. Deactivation can be minimized by hydrogen (in the presence of Pt) and water addition. Both measures are thought to reduce the concentration of intermediate olefins in the zeolite pores. The best results with respect to selective conversion of *n*-butane to isobutane were obtained for 0.25 wt% Pt on mordenite in the presence of hydrogen. Higher concentrations of Pt in the catalyst are shown to be detrimental for *n*-butane isomerization, because of increasing selectivity to hydrogenolysis. A detailed mechanistic scheme for *n*-butane conversion over Pt-containing mordenites is presented. *n*-Butane conversion is concluded to occur via a bimolecular mechanism involving a complex network of hydrogen transfer, oligomerization/cracking, isomerization, hydrogenation/dehydrogenation, and hydrogenolysis. © 1997 Academic Press

INTRODUCTION

The use of Brønsted acidic zeolites (e.g., H–mordenite) as a component of commercial *n*-butane isomerization catalysts has received much attention in both academic and industrial research (1–6). This is mainly due to the specific pore geometry combined with the strong acidic properties of these molecular sieves. We have shown earlier that *n*-butane conversion over H–mordenite occurs mainly via a bimolecular mechanism (3). For this bimolecular mechanism, two main reaction routes, isomerization (formation of isobutane) and disproportionation (i.e., formation of propane and pentane isomers), have been identified. The contribution to the two reaction routes depends upon the reaction temperature, the concentration of the acid sites, and the concentration of reactants in the pores of the catalyst (3).

The main problem associated with the use of strongly acidic zeolites as isomerization catalysts is the fast rate of deactivation. For the protonic form of mordenite, for example, the initial yields of isobutane are high. An optimal catalytic activity in the isomerization of *n*-butane (3) and *n*-pentane (4) was found for mordenite samples with a Si/Al ratio of 10. Blocking of the catalytic active sites by adsorbed (polymeric) hydrocarbons and partial pore blockage, however, cause loss of catalyst activity with time on stream.

Enhancement of the stability might be achieved by introducing additives into the feed stream which prevent the formation of polymeric hydrocarbons or help to decompose and desorb them (7). In this context, improved stability is expected by the addition of hydrogen to the feed stream, especially for catalysts containing low concentrations of Pt (8). The role of Pt has been reported to be in the activation of the hydrogen. The activated hydrogen is reported to react with the carbocationic intermediates, thus reducing their concentration in the zeolite pores (7, 11). This reduction in the concentration of the carbocations, however, might also cause a decrease in the rate of *n*-butane transformation as the carbocations are part of the catalytic cycle. Pt when present in a zeolite (MOR) or sulfated zirconia has also been suggested to contribute to the isomerization of butane via a parallel bifunctional route involving dehydrogenation of the alkane on the metal site (5, 6). As a side effect, the presence of Pt can also be expected to cause a new hydrogenolysis route in the presence of hydrogen thus affecting isobutane selectivity.

The beneficial use of water as additive to the hydrocarbon feed stream to reduce carbon formation has been reported for the skeletal isomerization of *n*-butenes over alumina catalysts (12, 13), and over W/Al_2O_3 (14). Water addition during pyridine adsorption on H–mordenite is claimed to decrease Lewis sites and to increase Brønsted acid sites. The effect was reversed when the added water was evacuated (15). While this might suggest that the role of water is to control the nature of the acid sites, it is also possible that water simply blocks some of the acid sites, thereby lowering the concentration of olefinic species (16) and hence oligomerization and coking.

The present contribution addresses the effect of the modification of H–mordenite with Pt and the addition of water and hydrogen to the feedstream on the activity, selectivity, and stability with the goal to understand and to be able to control the influence of these additives on the *n*-butane conversion over H–mordenite.

0021-9517/97 $25.00

TABLE 1

Physicochemical Characteristics of the Samples

Catalyst	BET surface area (m^2/g)	Pt content (wt%)	Pt dispersion (%)[a]	IR OH/latice vibration
HMOR	388	0	—	1.32
PtMOR1	226	0.02	[b]	1.15
PtMOR2	241	0.25	100	1.3
PtMOR3	259	1.3	80	1.1

[a] Measured by volumetric hydrogen chemisorption.
[b] Not measured.

EXPERIMENTAL

Catalyst Preparation and Characterization

H–mordenite (HMOR) with a SiO_2/Al_2O_3 ratio of 20 (provided by the Japanese Catalytic Society) was used in this study. A detailed characterization of the material is given in Ref. (17). Three different Pt/H–mordenite samples were prepared by contacting HMOR with a 1 *M* solution of $Pt(NH_3)_4Cl_2$ to obtain Pt loadings between 0.02 and 1.3 wt%. After contacting HMOR with the appropriate amounts of the Pt-salt solution for 1 h at ambient temperature under constant stirring, the solution was filtered, and the catalyst washed with deionized water. This material was dried overnight at ambient temperature and then at 383 K for 2 h. The dry powder was ground and calcined in air at 823 K. The samples are denoted PtMOR1, PtMOR2, and PtMOR3 corresponding to the Pt loadings of 0.02, 0.25, and 1.30 wt%, respectively. Dispersion of Pt in the samples was measured by volumetric hydrogen chemisorption. The IR spectra of the catalysts, to determine the concentration of –OH groups, were recorded using a Bruker IFS88 FTIR spectrometer. The physicochemical characteristics of these catalysts are shown in Table 1.

Kinetic Measurements

The catalytic tests were performed in a tubular quartz reactor operated in continuous flow mode. A catalyst loading of about 300 mg was used. The catalyst was diluted with inert quartz beads in the ratio of 1 : 1. A gas mixture of 20% *n*-butane in helium was used. The experiments were conducted between 523 and 623 K and with *n*-butane partial pressures between 74 and 150 mbar and at total pressures between 1.5 and 2.5 bar. The partial pressure of hydrogen was varied between 0 and 1500 mbar. Water was added by mixing the *n*-butane feed stream with a He stream that passed through a saturator containing water at room temperature. The required partial pressure of water was obtained by varying the temperature of the saturator and/or the flow rate of helium while keeping the total feed flow rate constant. Partial pressures of water of up to 15 mbar were used.

All catalysts were activated in flowing air by heating at 10 K/min to 823 K and holding this temperature for 1 h. For the Pt-containing catalysts an additional prereduction step was carried out at 823 K for 1 h in H_2. The reactant mixture was passed over the catalyst at space velocities between 0.8 and 1.5 ml/g ∗ s. The activity of the catalysts was monitored as a function of time on stream between 10 and 60 min. The reactor effluent was collected in the sample loops of a multiloop valve and subsequently analyzed by gas chromatography (HP 5890 with a 50-m Al_2O_3/KCl column, flame ionization detector).

RESULTS

Effect of Hydrogen on the Activity and Stability of H–Mordenite

The rate of conversion of *n*-butane at 523 K over H–mordenite as a function of time on stream at various H_2/*n*-butane ratios is depicted in Fig. 1. The main products in the conversion of *n*-butane over H–mordenite were isobutane ("isomerization route"), propane, and pentane isomers ("disproportionation route") as reported earlier (3). The addition of hydrogen to the *n*-butane feed led primarily to a decrease in the rate of *n*-butane conversion. The lower activity in the presence of hydrogen was also accompanied by a slower relative deactivation.

The selectivity to the main products was not significantly influenced by the increase in the H_2/*n*-butane ratio. The influence of hydrogen on the product distribution over H–mordenite is shown in Table 2. Only a slight increase in the selectivity to isobutane and pentane was noticed, while the selectivity to propane and to the cracking products methane and ethane slightly decreased. This can also

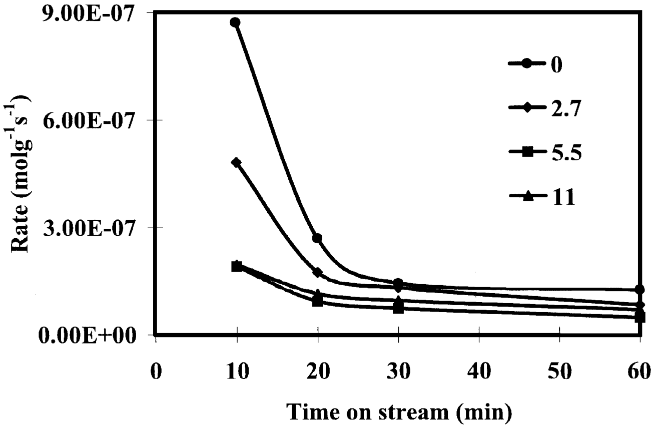

FIG. 1. Effect of hydrogen on the activity and stability of HMOR at 523 K. $P_{tot} = 2.5$ bar; $P_{n\text{-butane}} = 150$ mbar; flow rate = 15 ml/min; SV = 0.83 ml/g ∗ s; the values 0, 2.7, etc., indicate the H_2/*n*-butane ratios.

TABLE 2

Product Selectivity over HMOR and PtMOR3 at 523 K, Conversion = 5 mol%

	Selectivity (mol%)			
Catalyst:	HMOR		PtMOR3	
H_2/n-butane ratio:	0	11	0	11
Products				
Methane + ethane	1	1	0.5	61
Propane	34	31	33	31
Isobutane	53	55	52	7.5
Pentanes	11	12	13	0.4
C_{6+}	1	1	1.5	0

be seen in Fig. 2, in which the $iC_4/C_3 + C_5$ ratio is plotted against the H_2/n-butane ratio.

Effect of Platinum Loading on n-Butane Conversion

The effect of the Pt loading on the rate of conversion of *n*-butane (at 523 K) is shown in Fig. 3. It can be seen from Fig. 3 that the Pt-containing catalysts show higher catalytic activity than the parent H–mordenite. However, the presence of Pt did not lead to any improvement in the stability of the catalysts in the absence of hydrogen. The selectivity to various products for the different catalysts is shown in Fig. 4. With regard to the product distribution, only minor changes were observed upon Pt incorporation. A small increase in the selectivity to isobutane and a corresponding decrease in the selectivity to propane and pentane were the most significant changes over the Pt-containing catalysts in comparison to HMOR (Fig. 4, see also Fig. 2). In all cases low concentrations (<3%) of methane, ethane, and hexanes were also observed.

In the presence of hydrogen, however, a substantial decrease in the initial activity was observed with all the Pt-containing catalysts (see Fig. 5). It should be recalled that same was observed over H–mordenite (compare Figs. 3 and 5). However, the loss of activity in the presence of hydrogen was much more significant with Pt-containing catalysts than for HMOR at 523 K. The presence of hydrogen affected also the activity during time on stream. It can be seen from Fig. 5 that, in the presence of hydrogen, all catalysts reached steady state after 30 min on stream. In the absence of

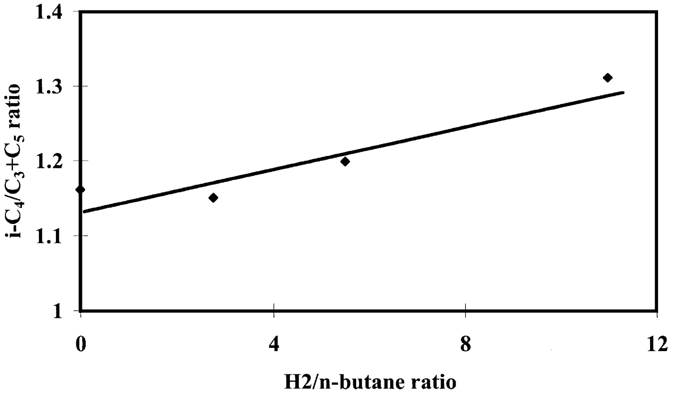

FIG. 2. Effect of hydrogen $iC_4/C_3 + C_5$ over HMOR at 523 K; $P_{tot} = 2.5$ bar; $P_{n\text{-butane}} = 150$ mbar; flow rate = 15 ml/min; SV = 0.83 ml/g ∗ s; conversion = 5 mol%.

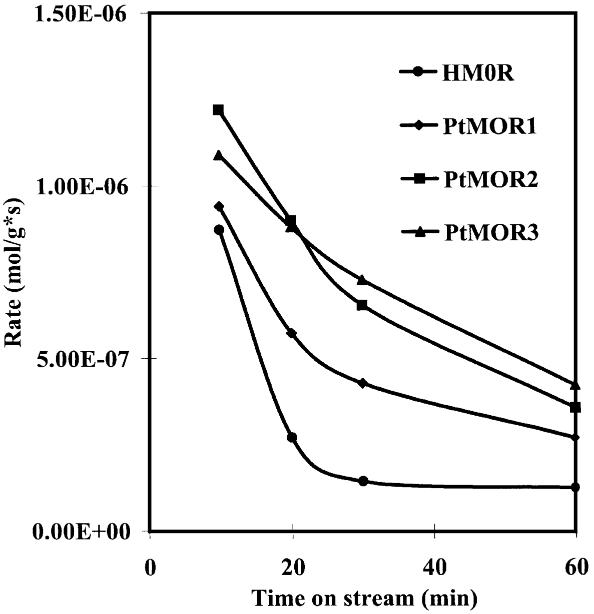

FIG. 3. Rate vs time on stream. Effect of Pt on activity and stability at 523 K; $P_{tot} = 2.5$ bar; $P_{n\text{-butane}} = 150$ mbar; flow rate = 15 ml/min; SV = 0.83 ml/g ∗ s.

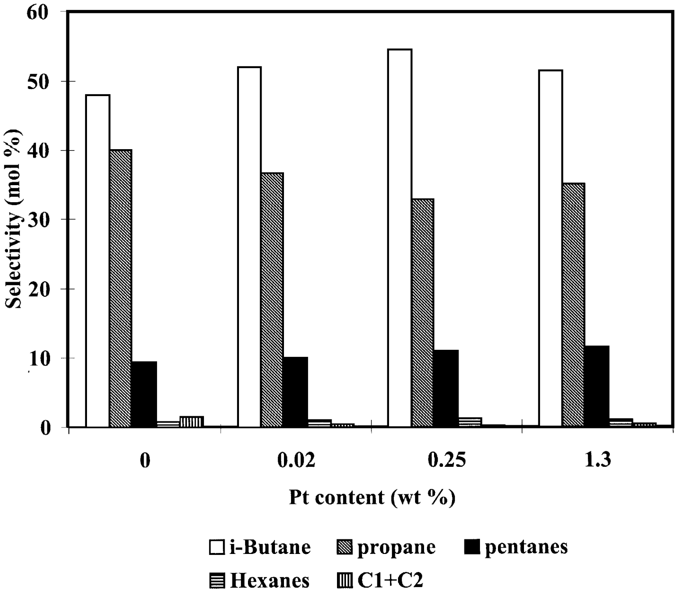

FIG. 4. Selectivity as a function of Pt loading at 20% conversion in the absence of hydrogen. $P_{tot} = 2.5$ bar; $P_{n\text{-butane}} = 150$ mbar; flow rate = 15 ml/min; SV = 0.83 ml/g ∗ s.

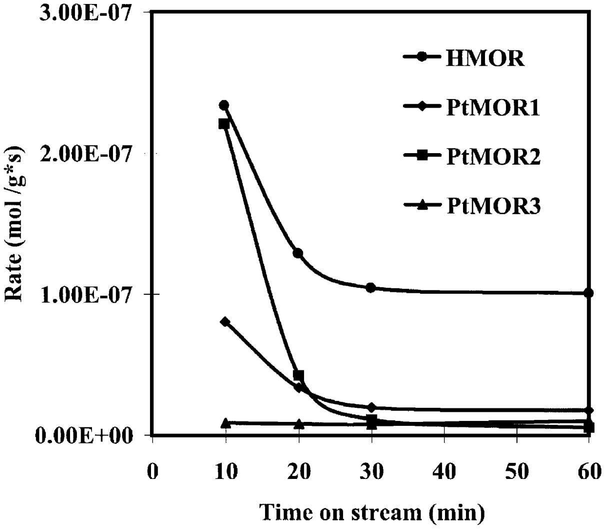

FIG. 5. Effect of Pt on activity and stability at 523 K in the presence of hydrogen. $P_{tot} = 1.5$ bar; $P_{n\text{-butane}} = 72$ mbar; flow rate = 20 ml/min; SV = 1.1 ml/g ∗ s; H_2/*n*-butane = 11.

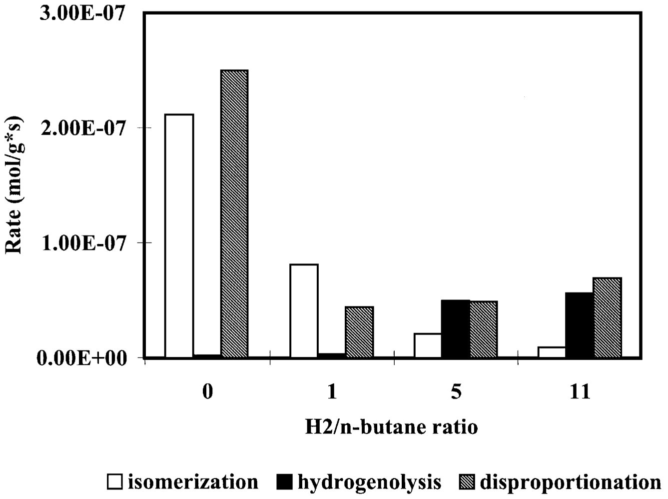

FIG. 6. Rate of reactions as a function of H_2/*n*-butane ratio over PtMOR3 at 523 K; $P_{tot} = 2.5$ bar; $P_{n\text{-butane}} = 150$ mbar; flow rate = 15 ml/min; SV = 0.83 ml/g ∗ s.

hydrogen, these catalysts continued to deactivate even after 60 min on stream (see Fig. 3). PtMOR3 which was the least active catalyst did not deactivate at all in the presence of hydrogen (Fig. 5). The influence of hydrogen on the product selectivity for HMOR and PtMOR3 is compiled in Table 2. For PtMOR3, the rates for isomerization (isobutane) and disproportionation (propane + pentanes) decreased, while the rates of hydrogenolysis (methane + ethane) increased in the presence of hydrogen. In contrast, in the case of H–mordenite, the presence of hydrogen did not cause any appreciable changes in selectivity. For Pt-containing catalysts, also similar product distribution to H–mordenite were observed in the absence of hydrogen (Fig. 4 and Table 2).

The relative contribution of the three main reactions (isomerization, disproportionation, and hydrogenolysis) to the total rate of conversion at 523 K is depicted as a function of H_2/*n*-butane ratio in Fig. 6 for PtMOR3. It can be seen that the presence of hydrogen induced a large negative effect on isomerization and disproportionation and a positive effect on hydrogenolysis at 523 K.

As already mentioned, the addition of hydrogen to enhance the stability of the catalyst led to lower rates of *n*-butane conversion over Pt containing catalysts. In order to improve the yields of isobutane, under practical reaction conditions it was necessary to work at temperatures higher than 573 K. The conversions and product distributions obtained over H–mordenite and two PtMOR samples at 623 K are summarized in Table 3. It can be seen from Table 3 that over Pt-containing catalysts an appreciable improvement in isobutane selectivity is observed. Even though Pt caused hydrogenolysis at higher temperatures, this was much less than at the lower temperature of 523 K (see Table 2). The stability of H–mordenite and Pt-mordenites in presence of hydrogen (H_2/*n*-butane = 15) at 623 K is presented as a function of time on stream in Fig. 7. In contrast to the lower activity (PtMOR1, PtMOR2, PtMOR3) and the fast initial deactivation (PtMOR1, PtMOR2) observed even in the presence of hydrogen at 523 K, a higher and stable activity was obtained for the Pt-mordenite samples at 623 K. However, even though H–mordenite deactivated under these conditions, it still had a better activity after 60 min on stream than the Pt containing catalysts.

Figure 8 shows the activity as a function of time on stream for PtMOR2 at varying H_2/*n*-butane ratios all lower than H_2/*n*-butane ratio of 15 shown in Fig. 7. It is evident from Fig. 8 that the stability of the catalysts is improved by an increasing H_2/*n*-butane ratio at the expense of catalytic activity. The results agree with those of Maness and Dooley for *n*-butane isomerization over fluorided Pd-mordenite (18). However, at the optimal H_2/*n*-butane ratio of 10 stable behavior combined with good activity is achieved.

The influence of H_2/*n*-butane ratio on the product distribution at about 50% *n*-butane conversion is shown in Fig. 9

TABLE 3

Product Distribution for *n*-Butane Conversion over Various Catalysts at 623 K, H_2/*n*-Butane Ratio = 15

	Selectivity at 50 mol% conversion		
Catalyst:	HMOR	PtMOR1	PtMOR2
Products			
Methane + ethane	4	8.7	17
Propane	53.7	34	23
Isobutane	33	48	52
Pentane	7	9	6.8
Others	2.3	0.3	1.2

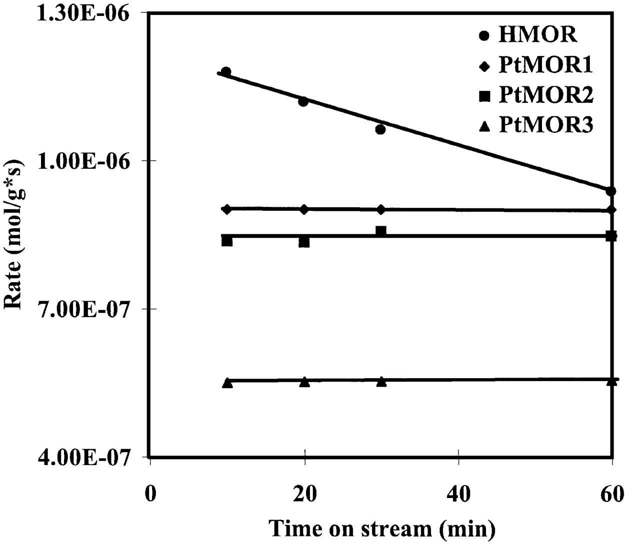

FIG. 7. Rate as a function of time on stream at 623 K for various catalysts, H_2/n-butane ratio = 15; $P_{tot} = 1.5$ bar; $P_{n\text{-butane}} = 74$ mbar; flow rate = 15 ml/min; SV = 1.13 ml/g ∗ s.

for PtMOR2. The selectivity to isobutane increased with increasing H_2/n-butane ratio, while the selectivity to propane showed the opposite trend. The extent of hydrogenolysis also increased with increasing H_2/n-butane ratio. The negative effect of hydrogen on the overall rate of n-butane conversion over PtMOR2 is depicted on Fig. 10. From the data displayed a negative order of 0.4 with respect to H_2 was calculated. In Fig. 11 the yield of products as a function of conversion is represented for PtMOR2. Under these conditions (H_2/n-butane = 20), catalyst deactivation was not observed during time on stream. It can be seen from Fig. 11 that propane is a primary and a secondary product. Isobutane and pentane which are also primary products are further converted to products.

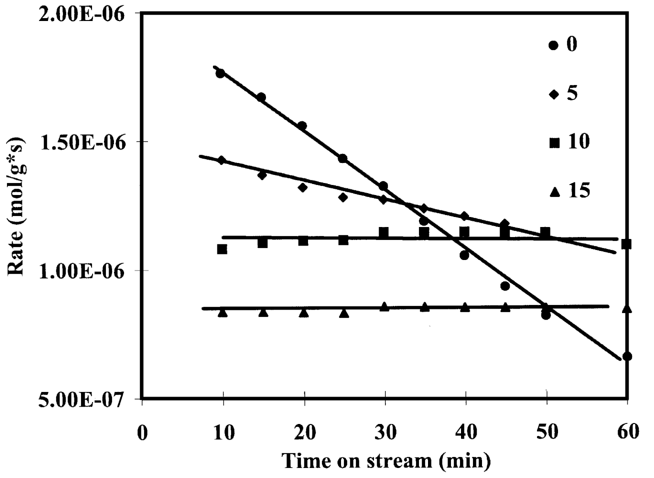

FIG. 8. Rate as a function of time on stream for various H_2/n-butane ratio over PtMOR2; $T = 623$ K; $P_{tot} = 1.5$ bar; $P_{n\text{-butane}} = 74$ mbar; flow rate = 20 ml/min; SV = 1.1 ml/g ∗ s.

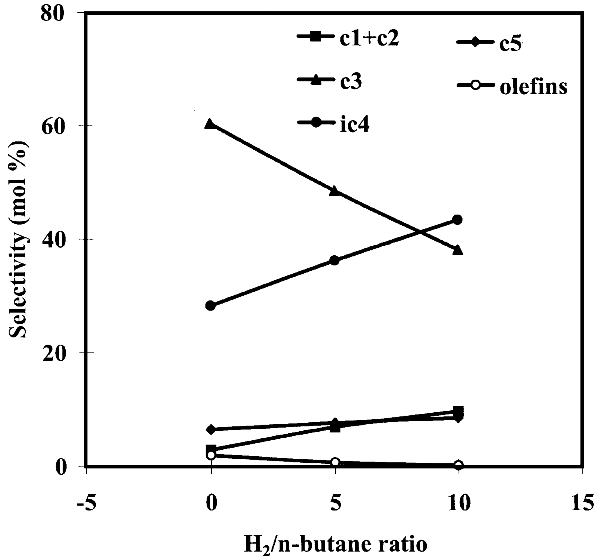

FIG. 9. Selectivity as a function of H_2/n-butane ratio at 50% conversion over PtMOR2. $T = 623$ K; $P_{tot} = 1.5$ bar; $P_{n\text{-butane}} = 74$ mbar; flow rate = 20 ml/min; SV = 1.1 ml/g ∗ s.

Effect of Water Cofeeding

Figure 12 shows the conversion over HMOR as a function of time on stream at 523 and 573 K in the presence and absence of water in the feed stream. The stabilizing effect of water is more obvious at 523 K. The effect of water cofeeding on the product distribution at 523 and 573 K over HMOR is summarized in Table 4. An increase in the selectivity to isobutane is observed, while the selectivity to propane decreased upon water cofeeding at 523 K. At 573 K water addition caused only subtle changes in selectivity.

Addition of water also had a positive effect on the stability of the Pt modified catalyst for n-butane conversion (Fig. 13). With respect to selectivity the presence of water caused only marginal changes at 523 K and none at 573 K (see Table 5).

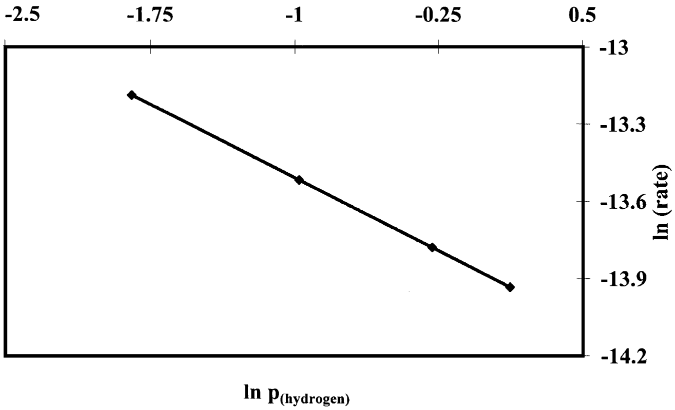

FIG. 10. Effect of hydrogen on the rate of n-butane conversion over PtMOR2 at 623 K.

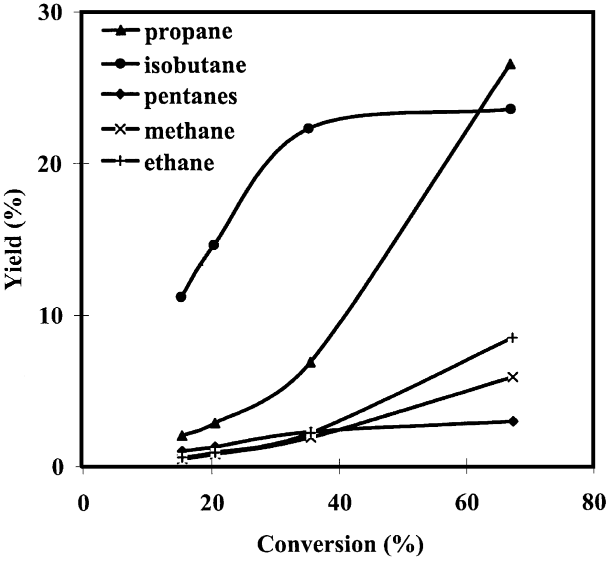

FIG. 11. Product yield as a function of conversion over PtMOR2 at 623 K; $P_{n\text{-butane}} = 75$ mbar; SV = 1.1 ml/g ∗ s.

DISCUSSION

We have shown earlier that over H–mordenites *n*-butane is mainly converted via a bimolecular mechanism at 523 K (3). This mechanism avoids the formation of the energetically unfavorable primary carbenium ions which are unavoidable, if isomerization occurs via a monomolecular skeletal isomerization route. We will show here that the results obtained over Pt-modified mordenites also point to a bimolecular reaction route. The proposed reaction network is shown in Fig. 14.

Two main reaction routes, isomerization (isobutane) and disproportionation (propane and pentane isomers), contribute to the product selectivity in the overall reaction.

TABLE 4

Effect of Water on Product Distribution during *n*-Butane Isomerization over HMOR at 523 and 573 K

	Selectivity at 20 mol% conversion (mol%)			
Temperature (K):	523		573	
Feed:	*n*-Butane	*n*-Butane + H_2O	*n*-Butane	*n*-Butane + H_2O
Products				
Methane + ethane	1.5	0	1	0.4
Propane	40	27	39	43.7
Isobutane	48	60	47.5	44
Pentanes	9.5	12	11	10.7
Others	0.8	1	1.5	1.5

Note. $P = 2.5$ bar; $p_{n\text{-butane}} = 150$ mbar; space velocity = 0.83 ml/g ∗ s; H_2O/*n*-butane ratio = 0.1.

It was shown earlier that the relative importance of the two reaction routes depends subtly upon the reaction temperature and the concentration of acid sites (3). In the biomolecular reaction sequence, *n*-butane is first protonated at the strong Brønsted acid sites to form a butyl carbonium ion. Subsequent dehydrogenation of this leads to a surface bound alkoxy group (carbenium ion) and hydrogen (initiation step). Note that it is now generally accepted that chemisorbed alkenes exist as alkoxy groups which on excitation form the carbenium ions in the transition state.

It is significant to recall at this point the negative half order (−0.4) in hydrogen observed for the rate of *n*-butane conversion. This suggests dissociation of hydrogen molecule as playing a part in the mechanism. Negative order in hydrogen has been observed recently and attributed as indication for a bifunctional mechanism (5)

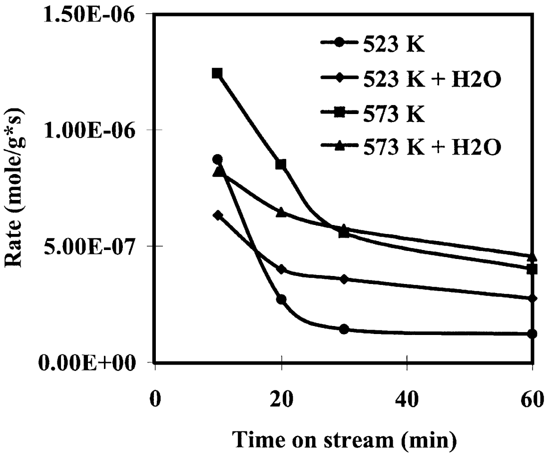

FIG. 12. Effect of water on the activity and stability of H–mordenite at 523 and 573 K; $P_{\text{tot}} = 2.5$ bar; $P_{n\text{-butane}} = 150$ mbar; flow rate = 15 ml/min; SV = 0.83 ml/g ∗ s.

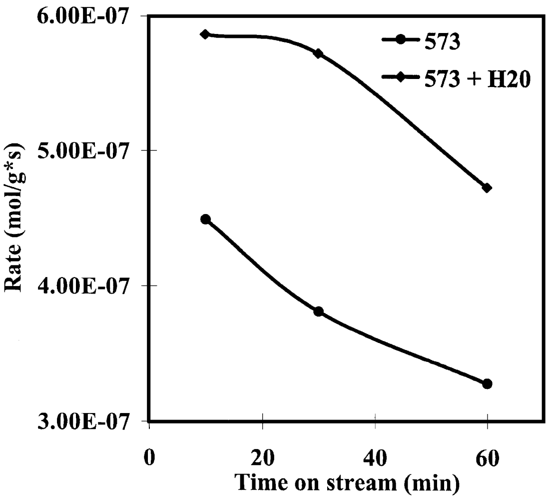

FIG. 13. Effect of water on the activity and stability of PtMOR2 at 573 K; $P_{\text{tot}} = 1.5$ bar; $P_{n\text{-butane}} = 74$ mbar; flow rate = 20 ml/min; SV = 1.1 ml/g ∗ s.

TABLE 5

Effect of Water on Product Distribution during *n*-Butane Conversion over PtMOR2 at 523 and 573 K

	Selectivity (mol%)			
Temperature (K):	523		573	
Feed:	*n*-Butane	*n*-Butane + H_2O	*n*-Butane	*n*-Butane + H_2O
Conversion (%):	6	4.9	20.4	21.5
Products				
Methane + ethane	0.1	0.6	0.5	0.5
Propane	20	22	32	33
Isobutane	67	66	55	54
Pentanes	11.6	10	11.2	11
C_{6+}	0.9	0.7	0.7	0.7
Olefins	0.4	0.7	0.6	0.8

Note. $P = 1.5$ bar; $p_{n\text{-butane}} = 72$ mbar; space velocity = 1.1 ml/g ∗ s.

involving dehydrogenation of butane at the Pt site and subsequent formation of butyl carbenium ion from the butene formed. It is, therefore, possible that in our expeirments an additional route for the formation butyl carbenium ion as in a bifunctional route exists (see Fig. 14).

The butyl carbenium ion may desorb as butene or react with another butene molecule to form an octyl carbenium ion. The octyl carbenium ion subsequently isomerizes and cleaves by forming *tert*-butyl carbenium ion and *n*-butene (isomerization route). The *tert*-butyl carbenium ions leave the catalyst surface as isobutane after abstracting a hydride from another *n*-butane feed molecule. In a second pathway the octyl carbenium ion undergoes oligomerization, cracking, and hydride transfer reactions to give propane and pentyl carbenium ion (disproportionation route). The pentyl carbenium ions crack to form propylcarbenium ions and some ethene or undergo hydride transfer reactions with reactant molecules before leaving the catalyst as alkanes (3).

It has been shown that the high hydride transfer ability of the H–mordenite causes the formation of almost exclusively saturated products (methane and ethane, propane, isobutane, *n*-butane, and pentanes) and coke upon conversion of *cis*-2-butene (19). The catalyst deactivates very rapidly during this experiment indicating that the extensive hydride transfer leaves increasingly hydrogen-deficient carbonaceous material on the catalyst surface. Similarly under the reaction conditions during *n*-butane isomerization, the formation of oligomeric, olefinic species is favored. These molecules will transform by hydrogen redistribution to form paraffins and increasingly carbon-rich and unreactive carbonaceous material. Their accumulation leads to the reduction of the catalytic activity with time on stream.

From the reaction network shown in Fig. 14, the lower activity of HMOR in the presence of hydrogen can be explained by a reduced rate of butene formation and, thus, also in butyl carbenium ions. This can be expected to reduce the overall rate of the reaction. A remarkable change in selectivity to various routes (disproportionation and isomerization) in the product distribution upon addition of hydrogen is neither expected nor seen. Thus, the selectivity to coke formation will also not change, although a slower coking rate will be expected as a result of reduced formation of olefins. The increased stability of H–mordenite in the presence of hydrogen is proposed to be due to the lower concentration of the olefins.

In the case of Pt-containing catalysts, paraffin isomerization is knwon to occur via a bifunctional mechanism involving the dehydrogenation of the paraffin on the metal, transport of the olefin to the acid site, isomerization of the alkenes at the acid site, followed by a hydrogenation of the iso-alkenes on the metal site to form iso-alkanes (20, 21). A mechanism involving protonated cyclopropane as intermediates in the monomolecular route for the isomerization of light paraffins has also been proposed. But this is limited to hydrocarbons with five or more carbon atoms that do not require the formation of primary carbenium ions for isomerization (21, 22).

The presence of hydrogen led to a reduction in the rate of *n*-butane conversion over Pt-mordenites just as in the case of H–mordenite. This negative effect of hydrogen upon the rate of the reaction was more drastic for Pt-containing catalysts than for H–mordenite at lower temperatures. This indicates that the formation of butenes is reduced. The addition of Pt is, thus, proposed to help in reducing the concentrations of butenes by controlling directly or indirectly their dehydrogenation.

The presence of hydrogen did not cause any change in the selectivity to different routes over H–mordenite. From the proposed mechanism, changes are not to be expected as the major reforming reactions will take place at the unmodified acid sites of mordenite. However, for the Pt-containing catalysts drastic changes are observed in the presence of hydrogen (Table 2 and Fig. 9). In the absence of hydrogen, the products obtained over the Pt-containing catalyst are similar to those over H–mordenite. Apart from the low concentration of cracking products observed, only a slight increase in the selectivity to isobutane and a decrease in the selectivity to propane is observed with increasing Pt loading. This suggests that Pt alone does not induce any major changes in the mechanistic pathway as seen over mordenite. We should recall at this point (see Table 1) that addition of Pt did not cause any appreciable changes to the acidity of mordenite.

In Pt/H–mordenites, the main role of Pt is to activate hydrogen and establish the butane/butene equilibrium. The hydrogen can react with the olefinic species in the mordenite pores and help in the formation of alkanes and this can be expected to cause a decrease in coke formation. The

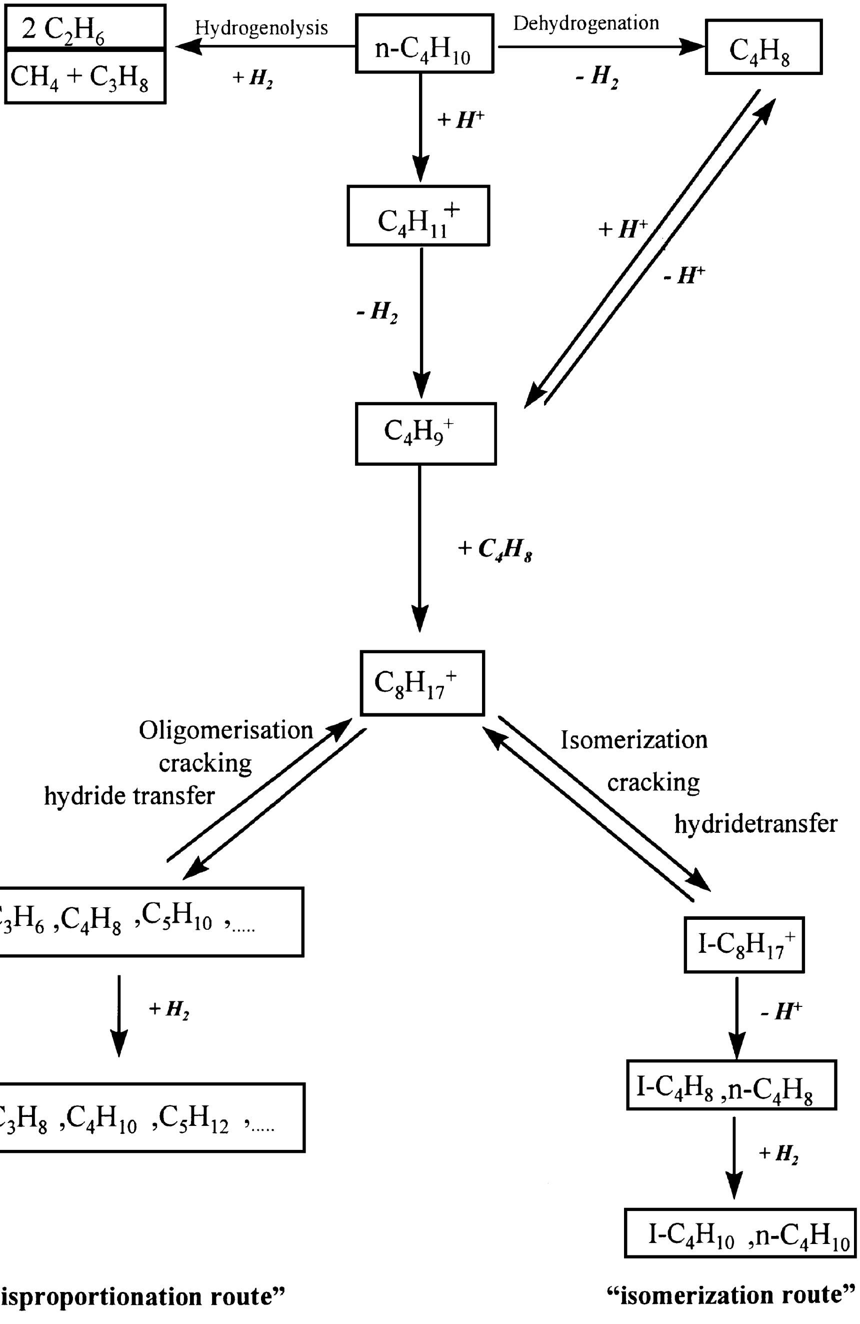

FIG. 14. Reaction pathways for *n*-butane isomerization over Pt–mordenites.

retardation of coking by hydrogen via reaction with benzylic carbocations has also been reported during toluene disproportionation over H–mordenites by Gnep and Guisnet (11). The reduction in the rate of conversion over Pt/mordenite is, thus, largely attributed to lower concentration of carbocations.

From the product distribution in Table 2, we conclude that the presence of H_2 caused hydrogenolysis, i.e., a high extent of $C_1 + C_2$ formation. Hydrogenolysis increases in importance with increasing Pt loading and H_2/*n*-butane ratio (Fig. 9), and at lower temperatures. In order to minimize the negative effects of hydrogenolysis, the reaction conditions needs to be subtly adjusted. An optimal H_2/*n*-butane ratio of 10, a Pt loading of 0.25%, and at 598 K gives the best results for *n*-butane isomerization.

Regarding the sequence of reactions over Pt containing catalysts, positives slopes for the yields (Fig. 11) at low conversion levels show that propane + pentane and isobutane are primary products formed in parallel ractions. Methane and ethane can be formed as primary products by hydrogenolysis of *n*-butane or as secondary products resulting from cracking of C_5 hydrocarbons. Propane has also very strong contribution from some secondary route.

The increase in the formation of propane with increasing conversion cannot be accounted for by the cracking of pentane to ethane and propane. This means that an additional route for the formation of propane exists. Because of the increase of methane and propane and the limiting value of isobutane yield at higher conversion we propose that oligomerization of isobutyl carbenium ion with a pentene occurs to form a C_9 species and subsequent cracking and hydride transfer will generate propane. Initially this hydride transfer should occur from *n*-butane. As the *n*-butane concentration decreases (i.e., at higher conversions) hydride transfer will occur preferably from isobutane. This explains the upper limit of 25 mol% isobutane yield. Note that it does not affect the other reactions occurring and as a consequence selectivity to isobutane will decrease at the expense of oligomerisation/cracking products. Dumesic *et al.* (23), proposed a microkinetic model to account for all the major products of isobutane conversion over acidic HY catalysts. The formation of excess propane during this reaction was accounted for by taking into account a secondary route involving C_4–C_4 and C_4–C_5 oligomerization and cracking steps. In this way propane was identified as both a primary and secondary product of isobutane conversion. The present experiments suggest that the additional secondary route propane is at the expense of isobutane formation. To summarize, with the present Pt mordenites, two routes, namely, hydrogenolysis of *n*-butane and oligomerization/cracking of tertiary butylcarbenium ion (precursor for isobutane) can cause losses in isobutane yield with increasing conversions.

Experiments with *cis*-butene conversion have also shown that coking occurs to a lesser extent in the presence of water over HMOR (17). This is explained with competitive adsorption of water on the acid sites of the catalyst blocking access for alkanes, i.e., acting like a diluent for acid sites. This will result in a lower concentration of chemisorbed olefins and, hence, a reduction in the rate of oligomerization and coking in parallel with a slight reduction in rate. Note that the stronger sorption of water is less important at higher temperatures (shift of sorption equilibria).

CONCLUSIONS

The mechanism of isomerization of *n*-butane over Pt-mordenites follows a bimolecular pathway as in the case of H–mordenite. In the presence of Pt an additional pathway for the conversion of *n*-butane via a bifunctional mechanism is also identified. Pt also induces high stability to the mordenite catalysts, which otherwise deactivate rapidly. The stability of Pt mordenites, especially in the presence of hydrogen, is achieved by suppressing coking, regulating the concentration of butene, and offering a pathway for alkene hydrogenation in addition to hydride transfer reactions. Under these conditions Pt catalysts hydrogenate the coke precursors. The presence of Pt, however, also causes hydrogenolysis of *n*-butane to methane, ethane, and propane. It has been shown that by the proper choice of reaction conditions, the route to hydrogenolysis could be minimized. Oligomerization/cracking of isobutane has been identified as a possible secondary route for the formation of propane. The presence of water in the reaction feed can also minimize coking rates and improve stability of mordenites, but the combined effect of Pt and hydrogen was far more effective.

ACKNOWLEDGMENTS

The Christian Doppler Laboratories of Heterogeneous Catalysis and OMV are acknowledged for the financial support of this work. We are grateful the Japanese Catalysis Society for providing the mordenite sample.

REFERENCES

1. Tonks, G. V., and Verstappen, A. E. L. M. M., U.S. Patent 5,073,667, 1991.
2. Mitsce, R. T., and Pollitzer, E. L., U.S. Patent 3,544,451, 1970.
3. Asuquo, R. A., Eder-Mirth, G., and Lercher, J. A., *J. Catal.* **155**, 376 (1995).
4. Tie, S. T., *Stud. Surf. Sc. Catal.* **85**, 587 (1994).
5. Liu, H., Lei, G. D., and Sachtler, W. M. H., *Appl. Catal. A: General* **137**, 167 (1996).
6. Chao, K., Hung-chung, W., and Leu, L., *J. Catal.* **157**, 289 (1995).
7. Polta, J. A., Flynn, D. K., and Thiel, P. A., *J. Catal.* **99**, 88 (1986).
8. Guisnet, M., and Fouche, V., *Appl. Catal.* **71**, 283 (1991).
9. Kouwenhoven, H. W., *Adv. Chem. Ser.* **121**, 529 (1973).
10. Benesi, H. A., and Winquist, B. H. C., *in* “Advances in Catalysis,” Vol 27. Academic Press, New York, 1978.
11. Gnep, N. S., and Guisnet, M., *Appl. Catal.* **1**, 329 (1981).
12. Butler, A. C., and Nicolaides, C. P., *Catal. Today* **18**, 443 (1993).
13. Myers, J. W., and Strope, D. J., U.S. Patent 4,436,949, 1984.
14. Gielgens, L. H., Ph.D. Thesis, Leiden University, The Netherlands, 1995.
15. Lefrancois, M., and Malbois, G., *J. Catal.* **20**, 350 (1971).
16. McVicker, G. B., Kramer, G. M., and Ziemiak, J. J., *J. Catal.* **83**, 286 (1983).
17. Sawa, M., Niwa, M., and Murakami, Y., *Zeolites* **10**, 532 (1990).
18. Maness, J. A., and Dooley, K. M., *J. Catal.* **117**, 322 (1989).
19. Asuquo, R. A., Seshan, K., and Lercher, J. A., submitted for publication, 1996.
20. Kuchar, P. J., Bricker, J. C., Reno, M. E., and Haizmann, R. S., *Fuel Proc. Tech.* **35**, 183 (1993).
21. Chevalier, F., Guisnet, M., and Maurel, R., “Proceedings, 6th International Congress on Catalysis, London, 1976” (G. C. Bond, P. B. Wells, and F. C. Tompkins, Eds.). The Chemical Society, London, 1977.
22. Bearez, C., Chevalier, F., and Guisnet, M., *React. Kinet. Catal. Lett.* **22**, 405 (1983).
23. Dumesic, J. A., Rudd, D. F., Apericio, L. M., Rekoske, J. E., and Trevino, A, A., *in* “The Microkinetics of Heterogeneous Catalysis,” p. 272. Am. Chem. Soc., Washington, DC, 1993.